Spontaneous Bacterial Keratitis in CD36 Knockout Mice

Spontaneous Bacterial Keratitis in CD36 Knockout Mice

Julia Klocke,[1] *Rita N. Barcia,*[1] *Susan Heimer,*[1] *Elke Cario,*[2] *James Zieske,*[1] *Michael S. Gilmore,*[1] *Bruce R. Ksander,*[1] *and Meredith S. Gregory*[1]

Purpose. CD36 is a Class B scavenger receptor that is constitutively expressed in the corneal epithelium and has been implicated in many homeostatic functions, including the homeostasis of the epidermal barrier. The aim of this study is to determine (1) whether CD36 is required for the maintenance of the corneal epithelial barrier to infection, and (2) whether CD36-deficient mice present with an increased susceptibility to bacterial keratitis.

Methods. The corneas of $CD36^{-/-}$, $TSP1^{-/-}$, $TLR2^{-/-}$, and C57BL/6 WT mice were screened via slit lamp microscopy or ex vivo analysis. The epithelial tight junctions and mucin layer were assessed via LC-biotin and Rose Bengal staining, respectively. Bacterial quantification was performed on corneal buttons and GFP-expressing *Staphylococcus aureus* was used to study bacterial binding.

Results. $CD36^{-/-}$ mice develop spontaneous corneal defects that increased in frequency and severity with age. The mild corneal defects were characterized by a disruption in epithelial tight junctions and the mucin layer, an infiltrate of macrophages, and increased bacterial binding. Bacterial quantification revealed high levels of *Staphylococcus xylosus* in the corneas of $CD36^{-/-}$ mice with severe defects, but not in wild-type controls.

Conclusions. $CD36^{-/-}$ mice develop spontaneous bacterial keratitis independent of TLR2 and TSP1. The authors conclude that CD36 is a critical component of the corneal epithelial barrier, and in the absence of CD36 the barrier breaks down, allowing bacteria to bind to the corneal epithelium and resulting in spontaneous keratitis. This is the first report of spontaneous bacterial keratitis in mice. (*Invest Ophthalmol Vis Sci.* 2011;52:256–263) DOI:10.1167/iovs.10-5566

Although *Staphylococci* are found in the normal flora of the ocular surface, mice are highly resistant to infection and do not develop spontaneous bacterial keratitis. Resistance to a corneal infection is dependent on the presence of multiple barriers that prevent bacterial adhesion and invasion. The disruption of any one of these barriers increases significantly the susceptibility to infection. Two of the critical barriers are the mucin layer, which prevents bacterial binding to the cornea, and the intercellular tight junctions of the corneal epithelium, which prevent bacterial penetration into the cornea.[1,2] In the normal cornea, these barriers effectively prevent infection. However, a disruption of these barriers due to injury or disease significantly increases the risk of bacterial keratitis.

CD36 is a Class B scavenger receptor that is expressed on multiple cell types, and recently it was found expressed constitutively on the corneal epithelium.[3–5] CD36 has multiple ligands, including TSP1, oxidized LDLs, oxidized phospholipids, and apoptotic cells.[4] As a pleiotropic ligand, CD36 has been implicated in multiple homeostatic and pathologic functions, including angiogenesis, atherosclerosis, phagocytosis, inflammation, lipid metabolism, and uptake of apoptotic cells.[3] Recently Hardy and colleagues[4] demonstrated that CD36 prevents corneal neovascularization and helps maintain the avascularity of the cornea. Furthermore they report that $CD36^{-/-}$ mice develop spontaneous corneal neovascularization that increases in severity with age.[5] However, our data suggest that the neovascularization is not spontaneous but is actually secondary to corneal defects that occur in the epithelium of aged $CD36^{-/-}$ mice.

Herein we report that $CD36^{-/-}$ mice develop spontaneous bacterial keratitis with age. Furthermore, the development of bacterial keratits is secondary to the breakdown of two critical components of the corneal epithelial barrier to infection: the mucin layer and epithelial tight junctions. Mice are normally highly resistant to bacterial keratitis, and this is the first report of spontaneous keratitis developing in a mouse from resident flora, highlighting a novel function for CD36 in maintaining the corneal epithelial barrier to infection.

Methods

Animals

Female C57BL/6 WT mice were purchased from the Jackson Laboratory (Bar Harbor, ME). The $CD36^{-/-}$ (C57BL/6 background) mice were originally received from Kathryn J. Moore (Massachusetts General Hospital, Harvard Medical School, Boston, MA).[6,7] The $TSP1^{-/-}$ mice (C57BL/6 background) were originally received from Jack Lawler (BIDMC, Harvard Medical School, Boston, MA).[8] All mice were bred and maintained in a pathogen-free facility at Schepens Eye Research Institute and provided with autoclaved tap water and autoclaved standard laboratory chow ad libitum. All animals were treated according to the Association for Research in Vision and Ophthalmology Resolution on the Use of Animals in Research. The Schepens IACUC committee approved all procedures involving mice. Elke Cario provided enucleated eyes from $TLR2^{-/-}$ mice (Tlr2tm1Kir; F10 [C57BL6/J]) housed under pathogen-free conditions at the Central Animal Facility of University Hospital of Essen. All animals were treated in compliance with German law for use of live animals and approved by the Institutional Animal Care and Use Committee at the University Hospital of Essen and the responsible district government.

From the [1]Schepens Eye Research Institute, Department of Ophthalmology, Harvard Medical School, Boston, Massachusetts; and [2]Division of Gastroenterology and Hepatology, University Hospital of Essen, and Medical School, University of Duisburg-Essen, Essen, Germany.

Supported by Research to Prevent Blindness Sybil B. Harrington Scholar Award (MSGr), EY016486 (BRK), EY017381 (MSGi), and DFG CA226/4-2 (EC).

Submitted for publication March 22, 2010; revised May 5, 2010; accepted August 3, 2010.

Disclosure: **J. Klocke**, None; **R.N. Barcia**, None; **S. Heimer**, None; **E. Cario**, None; **J. Zieske**, None; **M.S. Gilmore**, None; **B.R. Ksander**, None; **M.S. Gregory**, None

Corresponding author: Meredith S. Gregory, Schepens Eye Research Institute, 20 Staniford Street, Boston, MA 02114; meredith.gregory@schepens.harvard.edu.

Clinical Scoring

A one-time slit lamp examination was performed on each eye of every mouse in our C57BL/6 WT ($n = 87$), CD36$^{-/-}$ ($n = 90$), and TSP1$^{-/-}$ ($n = 83$) colonies. An additional subset of CD36$^{-/-}$ mice ($N = 8$) was used to study disease progression and as such were monitored monthly via slit lamp examinations for 13 months. After slit lamp examination, the eyes were placed into three categories: (1) no corneal defect, clear cornea; (2) mild corneal defect, mild corneal haze in which the iris is still visible; and (3) severe corneal defect, corneal opacity and neovascularization in which the iris is not visible. Enucleated eyes from TLR2$^{-/-}$ mice ($N = 8$ mice) were examined ex vivo using a dissecting microscope.

Histologic Analysis

Mice were euthanatized, and one group of eyes was enucleated, fixed in 10% buffered formalin, embedded in paraffin, sectioned, and stained with hematoxylin and eosin (H&E). A second group of eyes was enucleated and snap-frozen (Tissue-Tek OCT compound; Sakura Finetek, Torrance, CA). The frozen eyes were sectioned at 12-μm increments and stored at −20°C until ready for use. Macrophages were detected using a rat anti-mouse F4/80 antibody (Caltag, Burlingame, CA). Neutrophils were detected using a rat anti-mouse Ly-6 (GR1) antibody (Pharmingen, San Diego, CA) followed with a Cy3-conjugated goat anti-rat IgG_{2b} antibody (Jackson Laboratories, West Grove, PA). Purified rat IgG_{2b} was used as an isotope control (Pharmingen). A cyanine nucleic acid stain (To-Pro-3; Molecular Probes, Eugene, OR) was used to stain all cells. After immunostaining, tissue sections were mounted (VectaShield Mounting Medium; Vector Laboratories, Burlingame, CA), protected with coverslips, and stored at 4°C until analyzed by confocal microscopy. Immunostained tissue sections were analyzed using a confocal laser scanning microscope (TCS 4D; Leica, Wetzler, Germany). Gram staining was performed on paraffin-embedded tissues using a Gram stain kit according to the manufacture's protocol (Becton Dickinson Co., Franklin Lakes, NJ).[9]

Bacterial Quantification and Identification

To quantify bacterial load in corneas from CD36$^{-/-}$ mice with either no corneal defects, mild defects, or severe defects, we enucleated the eyes, and removed the corneas in a sterile environment. Each cornea was minced with a sterile blade and transferred into an Eppendorf tube containing 100 μL sterile PBS. Cultures were plated on BHI agar plates (Bacto Brain and Heart Infusion and Difco agar; Becton Dickinson, Franklin Lakes, NJ) and grown at 37°C overnight. Colonies were counted the following day. Five representative single colonies from each BHI plate were streaked for identification (BBL Chromagar Orientation agar plates; Becton Dickinson) and incubated at 37°C overnight. The bacterial species were preliminarily identified based on colony color (opaque pink) as described in the manufacturer's guidelines (Becton Dickinson).

16S rRNA Sequencing and Analysis

For 16S rRNA gene sequence identification, single colonies from each BHI agar plate (five representative colonies) were suspended in 50 μL sterile water, and a colony PCR was performed using 16S rRNA gene eubacterial oligonucleotide primers 27F and 1429R (Integrated DNA Technologies, Coralville, IA) as previously described.[10] PCR products were confirmed by electrophoresis through a 1% agarose gel and visualized by ethidium bromide staining. The 16S rRNA amplicons were sequenced by the DNA Sequencing Center for Vision Research at the Ocular Molecular Genetics Institute, Massachusetts Eye and Ear Infirmary (BigDye Terminator v3.1 cycle sequencing Ready Reaction mixture; Applied Biosystems, Foster City, CA). All 16S rRNA sequences were compiled using Basic Local Alignment Search Tool (BLAST) analysis.

Rose Bengal Staining

The corneal mucin layer was assessed in CD36$^{-/-}$ and C57BL/6 WT mice using a slightly modified Rose Bengal staining protocol that was originally developed for rabbits.[11] Briefly, Rose Bengal (Sigma-Aldrich, St. Louis, MO) was diluted in sterile saline to make a 0.1% solution. One drop of Rose Bengal was applied to the cornea of anesthetized mice. After one minute of incubation, the drop of Rose Bengal was removed by carefully placing a sponge at the limbus to absorb the excess dye without damaging the corneal surface. The eyes were examined under a slit lamp (Topcon Cooperation, Tokyo, Japan) using white light, and representative pictures were taken.

LC-Biotin Staining

The integrity of the corneal epithelial tight junctions was assessed in CD36$^{-/-}$ and wild-type (WT)-C57BL/6 mice using the LC-biotin staining method as described previously.[12,13] Briefly, 1 mg/mL stain (EZ-Link-Sulfo-NHS-LC-Biotin; Pierce, Rockford, IL) was dissolved in a salt solution (Hank's Balanced Salt Solution; Lonza, Walkersville, MD) with 2 mM $MgCl_2$ and 1 mM $CaCl_2$.[13] At the time of euthanatization, one drop of LC-biotin was applied to each eye. After 15 minutes, the eyes were rinsed with PBS and enucleated. Eyes were frozen on dry ice (Tissue-Tec O.C.T Compound; Sakura Finetek), and 8 μm sections were cut using a cryostat. The sections were fixed in acetone, blocked with 1% BSA (bovine serum albumin, Sigma- Aldrich), and incubated with fluorescein isothiocyanate (FITC)-conjugated streptavidin (1:50 in 1% BSA) and a nuclear dye (TO-PRO-3, 1:1000 in PBS; Invitrogen, Carlsbad, CA) for 1 hour at room temperature. The stained sections were mounted (Vectashield Mounting Medium for Fluorescein; Vector Laboratories), and examined with a confocal laser-scanning microscope (Leica Microsystems).

Staphylococcus aureus Binding Assay

To visualize bacterial binding to the cornea, a GFP- expressing strain of *S. aureus* (ALC 1435) was used. *S. aureus* ALC 1435 is a derivative of RN6390 containing the plasmid pALC1420 encoding GFP, whose constitutive expression is controlled through the *sar* P1 promoter.[14] Here 5 mL BHI (Bacto Brain and Heart Infusion; Becton Dickinson) was inoculated with a single colony of ALC 1435 isolated from a BHI agar plate and grown statically at 37°C overnight until the estimated density of 1×10^8 colony forming units [CFUs]/mL was reached. After 17 hours of static growth the culture was diluted 1:25 in BHI and grown shaking (200 rpm) until reaching an estimated density of 5×10^7 CFUs/mL or $OD_{595} = 0.22 \times 2$. The bacteria were pelleted, washed twice with PBS, and resuspended in 10 mL PBS. To assess bacterial binding, freshly enucleated eyes were incubated with 1×10^8 CFUs of the GFP-ALC1435 in a 48-well plate for 30 minutes at 37°C. After incubation the eyes were washed twice with PBS. The corneas were then excised in a sterile environment, mounted (Vectashield Mounting Medium for Fluorescein; Vector Laboratories), and examined under a confocal laser-scanning microscope (Leica).

Statistical Analysis

The appearance of corneal defects in CD36$^{-/-}$ mice was statistically analyzed using Fisher's exact test. This test was also used to analyze the bacterial load in corneas with and without severe defects. Significance was determined at $P < 0.05$. The relationship between age and the development of corneal defects was analyzed using proportional odds logistic regression (LogXact v.8; Cytel Inc., Cambridge, MA).

Results

Age-Related Development of Corneal Defects in CD36$^{-/-}$ Knockout Mice

Similar to the corneal epithelium, a critical function of the epidermis of the skin is to provide a barrier between the

external environment and the organism. Furthermore, CD36 has been shown to play a critical role in both maintaining the epidermal barrier and restoring the barrier after injury.[15,16] Therefore, we tested the hypothesis that the spontaneous development of corneal opacity and neovascualrization in $CD36^{-/-}$ mice[5] is due to a breakdown in the epithelial barrier, rendering the cornea more susceptible to infection.

To determine the frequency and severity of corneal defects in $CD36^{-/-}$ mice, we performed a slit lamp examination of each mouse in our $CD36^{-/-}$ ($N = 90$) and WT-C57BL/6 ($N = 87$) colonies. The age of mice at the time of examination ranged from 2 to 16 months in both colonies. After examination the eyes were placed into three categories: (1) no corneal defect, clear cornea; (2) mild corneal defect, mild corneal haze through which the iris is visible; and (3) severe corneal defect, corneal opacity and neovascularization through which the iris is not visible. All the WT-C57BL/6 mice, regardless of age, presented with normal clear corneas (Figs. 1A and 1C). By contrast, the $CD36^{-/-}$ mice presented with mild corneal defects as early as 2 months old at a frequency of 7% (2/28). The frequency of mild corneal defects increased significantly with age, and in 16-month-old $CD36^{-/-}$ mice the frequency of mild corneal defects was 60% (12/20) (Figs. 1A and 1B). The severe corneal defects first appeared at 6 months of age and increased in frequency to 40% (8/20) in 16-month-old $CD36^{-/-}$ mice. Moreover, monthly monitoring of a subset of $CD36^{-/-}$ mice revealed the development of mild defects always preceded the development of severe defects (Fig. 1D). Overall, the frequency and severity of mild and severe corneal defects observed in $CD36^{-/-}$ mice increased with age, and by 16 months 100% of $CD36^{-/-}$ mice displayed either mild or severe defects (Figs. 1B and 1D). There was a statistically significant relationship between increasing age and the presence of corneal defects in $CD36^{-/-}$ mice compared with controls as determined by proportional odds logistic regression (beta = -0.3652, $P = 5.005 \times 10^{-8}$). We conclude that $CD36^{-/-}$ mice spontaneously develop corneal defects that increase in frequency and severity with age.

Histologic Analysis of Corneal Defects in $CD36^{-/-}$ Mice

Histologic analysis and immunofluorescence was performed to identify the histologic changes that coincide with the mild and severe defects. H&E staining of clear corneas isolated from young $CD36^{-/-}$ mice revealed a normal corneal epithelium, stroma, and endothelium (Figs. 2A and 2B). Mild corneal defects coincided with the presence of disorganized apical epithelial layers, thickened basement membrane, and an infiltrate into the apical stroma just under the epithelial defect (Figs. 2A and 2B). Severe defects coincided with the presence of significant epithelial damage and a massive inflammatory infiltrate throughout the cornea (Figs. 2A and 2B). Interestingly, immunofluorescence revealed an increased number of F4/80 macrophages in "clear" (no defects visible) corneas from young $CD36^{-/-}$ mice compared with WT-C57BL/6 mice (Fig. 2C). The numbers of macrophages increased with the severity of the defect and were localized to the site of the corneal defect. By contrast, neutrophils were detected only in corneas with severe defects (Fig. 2D). The histology of the severe corneal defects is consistent with the histology observed in bacterial keratitis.[17,18] Therefore, the next series of studies were performed to determine whether bacteria were present in the corneas with severe lesions.

Bacterial Quantification

Bacterial quantification was performed to determine whether the severe corneal defects coincided with bacterial keratitis. Two methods were used to detect the presence of bacteria within the corneal tissue: Gram stain and enumeration of

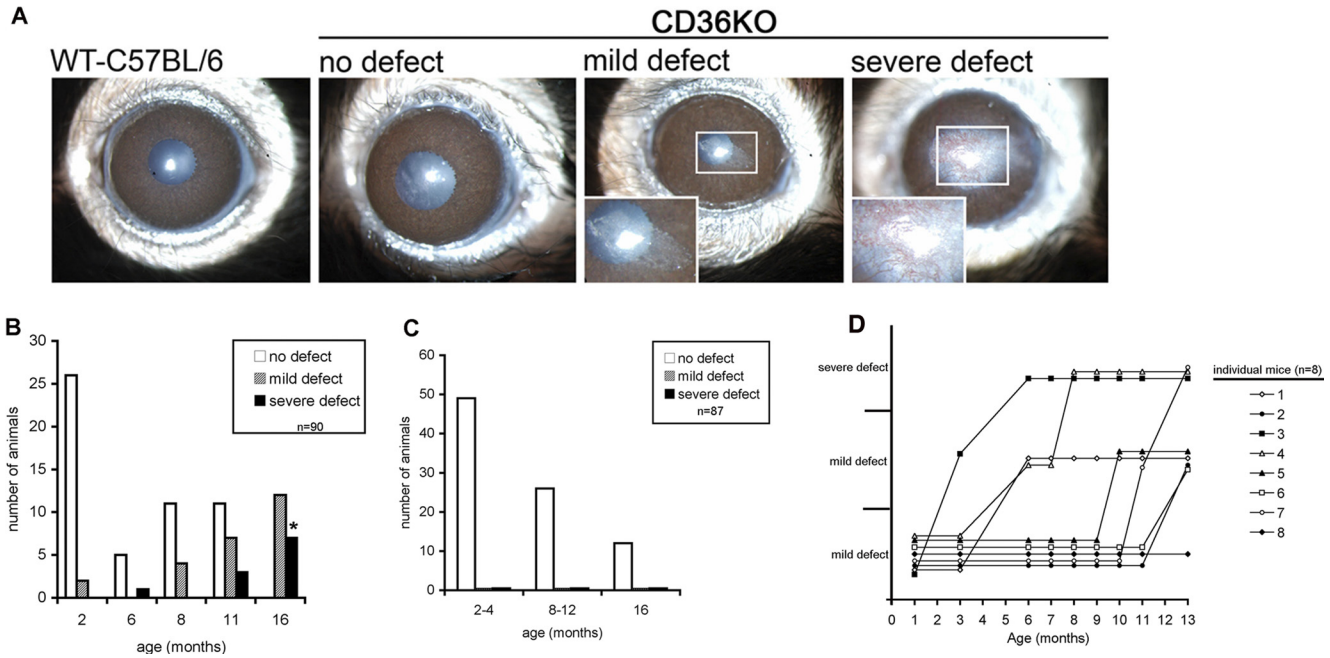

Figure 1. $CD36^{-/-}$ mice spontaneously developed corneal defects that increase in frequency and severity with age. (**A**) Slit lamp pictures of representative eyes from of $CD36^{-/-}$ mice that display (1) no corneal defect, clear cornea; (2) mild corneal defect, mild corneal haze through which the iris is visible; and (3) severe corneal defect, corneal opacity, and neovascularization through which the iris is not visible. (**B**) The frequency of corneal defects in $CD36^{-/-}$ mice ($n = 90$). (**C**) Age-matched WT C57BL/6 mice served as a negative control ($n = 87$). (**D**) Disease progression was monitored monthly in a subset of $CD36^{-/-}$ mice ($n = 8$). Asterisk indicates significant difference in the frequency of severe lesions between 16-month-old $CD36^{-/-}$ and WT-C57BL/6 mice ($P = 1.745 \times 10^{-9}$) and was determined by Fisher's exact test. Development of corneal defects in $CD36^{-/-}$ mice was age dependent as determined by proportional odds logistic regression (beta = -0.3652, $P = 5.005 \times 10^{-8}$).

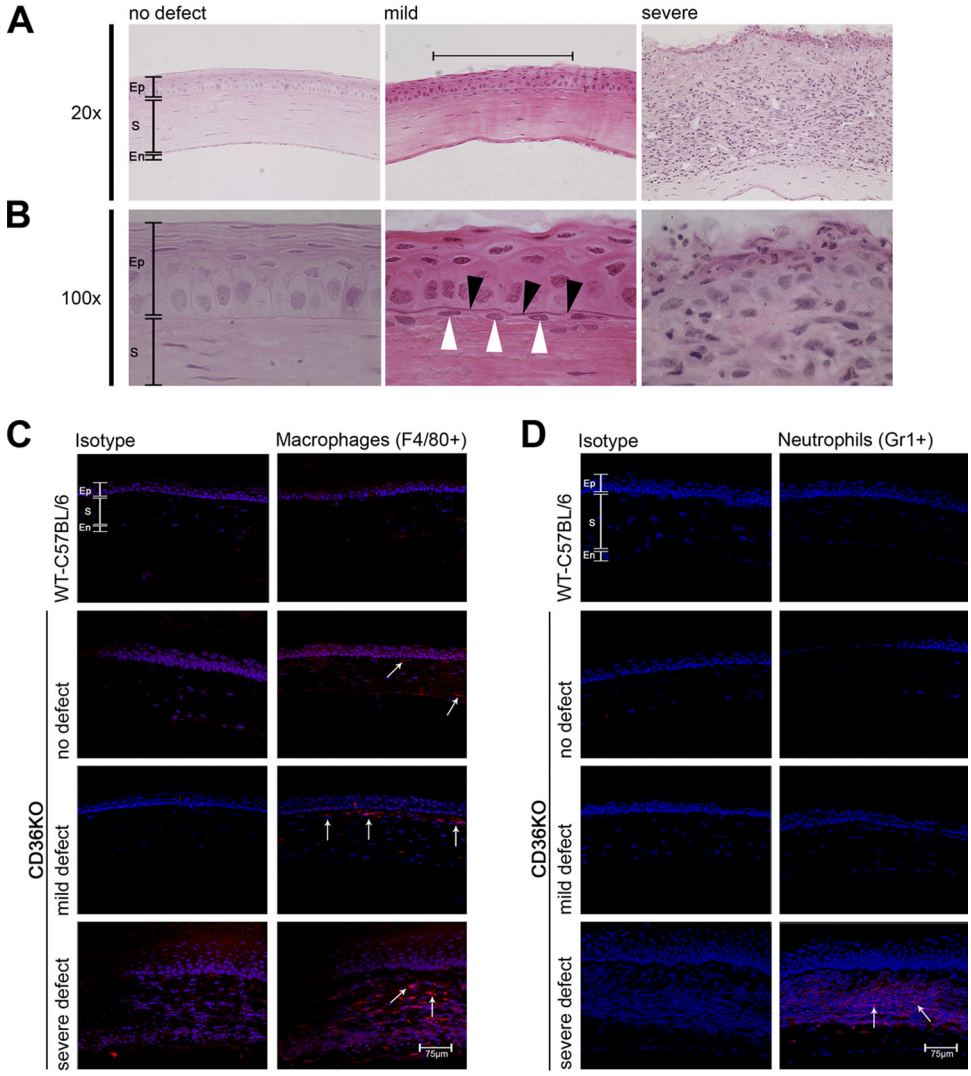

FIGURE 2. Histology of corneal defects. Corneas were recovered from mice with no defects, young CD36$^{-/-}$ mice; mild defects; or severe defects. (**A**, **B**) Corneas were fixed, paraffin embedded, sectioned, and stained with hematoxylin and eosin. (**C**) Corneas were recovered from WT C57BL/6 mice or CD36$^{-/-}$ mice with either no defect, mild defect, or severe defects. Corneas were snap frozen in OCT, sectioned, and stained with either an isotype-matched control antibody or an anti-F4/80 antibody (specific for macrophages). (**D**) A similar set of corneal sections were stained with either an isotype-matched control antibody or an anti-GR1 antibody (specific for neutrophils). All sections were stained with a cyanine nucleic acid stain (*blue*) to identify the cell nucleus. Immunofluorescence was examined via confocal microscopy. Ep, epithelium; S, stroma; En, endothelium. *Black arrowheads* identify a thickened basement membrane. *White arrowheads* identify a stromal infiltrate directly under the mild corneal defect. *White arrows* identify F4/80- and GR1-positive cells.

bacterial colonies from corneal tissue. Gram staining was performed on CD36$^{-/-}$ corneas with no defect, mild defects, and severe defects (Fig. 3A). No bacteria were detected by Gram stain in corneas with either no defects or mild defects. By contrast, a large amount of Gram-positive bacteria (dark purple) were detected in severe corneal defects (Fig. 3A). Higher magnification revealed individual cocci indicative of Gram-positive bacteria. Bacteria present in the corneas of WT-C57BL/6 and CD36$^{-/-}$ mice with no defect, mild defect, or severe defect were quantified by plate count. Bacterial quantification revealed large numbers of bacteria (>1000 CFUs) in 75% of the CD36$^{-/-}$ corneas with severe defects (Fig. 3B). Moderate colonization (<1000 CFUs) of 25% of CD36$^{-/-}$ corneas with severe defects as well as 25% of corneas with mild defects was observed. There was a statistically significant difference in the frequency of corneas with a high bacterial load in mice with severe lesions compared with either (1) wild-type corneas or (2) corneas from young CD36$^{-/-}$ mice with no defects. (Fisher's exact test, significance $P = 0.01$). Representative colonies grown on BHI plates from corneas with severe defects were cultured (BBL Chromagar orientation plates; Becton Dickinson) and produced opaque pink colonies, indicative of *Staphylococci* (data not shown). In addition, 16s ribosomal RNA sequencing and BLAST analysis in GenBank revealed a 99% homology to *Staphylococcus xylosus,* a commensal bacterium on the skin of humans and rodents (data not shown)[19,20].

Corneal Defects in TSP1$^{-/-}$ and TLR2$^{-/-}$ Mice

CD36 is a member of the class B scavenger receptor family with multiple functions.[3–5] Previous studies demonstrated that CD36 inhibited neovascularization through the binding of thrombospondin-1 (TSP1) and activation of anti-angiogenic pathways.[4] In addition, CD36 acts as a co-receptor for TLR2 and is required for the internalization of *S. aureus* and initiation of TLR2/6 signaling.[7] Therefore, the development of bacterial keratitis in CD36$^{-/-}$ mice may be due to inhibition of the TSP1 and/or TLR2 signaling pathway. To determine whether corneal defects develop in CD36$^{+/+}$ mice that lack either TSP1 or TLR2, we examined the corneas of TSP1$^{-/-}$ and TLR2$^{-/-}$ mice. Clinical examination and histologic analysis revealed no corneal defects in TSP1$^{-/-}$ or TLR2$^{-/-}$ mice up to 25 months of age (Table 1). In CD36$^{-/-}$ mice, 38% (14/36) of the mice present with either a mild or severe corneal defect by 11 months of age. By contrast, 0% (0/43) of the TSP1$^{-/-}$ mice displayed any corneal defects. Furthermore, 100% (20/20) of the CD36$^{-/-}$ mice present with a mild or severe corneal defect by 16 months of age, while 0% (0/8) of the TLR2$^{-/-}$ mice present with any corneal defects at 25 months of age. These results indicate

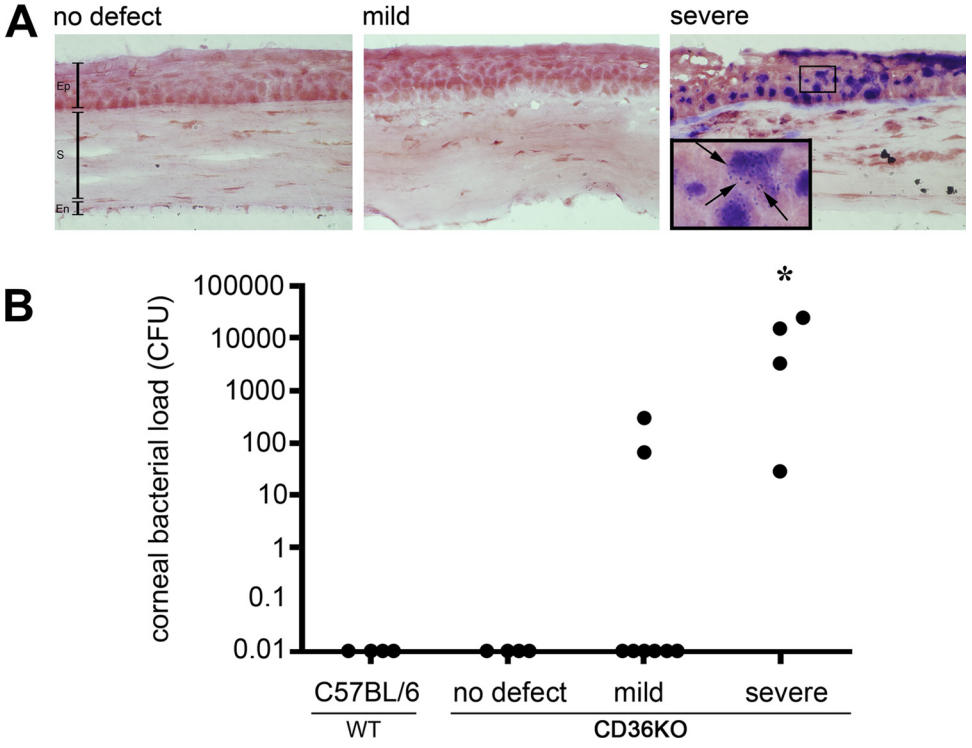

FIGURE 3. Detecting bacteria in corneal defects. Corneas were recovered from WT-C57BL/6 mice or CD36$^{-/-}$ mice with either no defects, mild defects, or severe defects. (**A**) Corneal sections were stained with a Gram stain. Gram-positive bacteria (*dark purple*) were detected in corneas with severe lesions. Pictures are representative of corneas from at least three different mice. (**B**) The bacterial load within individual corneas was determined by homogenizing and culturing the corneal tissue in BHI agar cultures. Bacterial colonies were enumerated and the CFUs for each cornea displayed [n = 4 (C57BL/6), n =4 (no defect), n = 8 (mild defect), n = 4 (severe defect)]. *Asterisk* indicates significant increase in bacterial load compared with all other groups (Fisher's exact test, P = 0.01). Ep, epithelium; S, stroma; En, endothelium. *Black arrows* identify Gram-positive cocci.

that the spontaneous corneal defects that occur in CD36$^{-/-}$ mice are independent of either TSP1 or TLR2 pathway.

Rose Bengal Staining in CD36$^{-/-}$ Mice

The mucin layer is a major component of the ocular tear film involved in preventing bacterial adherence to the cornea.[1] Rose Bengal staining was used to determine whether the mild and/or severe corneal defects coincided with a disruption in the mucin layer.[21] An intact mucin layer prevents positive Rose Bengal staining in healthy eyes.[22] By contrast, increased Rose Bengal staining coincides with the disruption of the mucin layer.[23] Rose Bengal staining was negative in C57BL/6 WT eyes and CD36$^{-/-}$ corneas with no corneal defects (Fig. 4A). By contrast, positive Rose Bengal staining was observed in CD36$^{-/-}$ corneas with either mild or severe defects. Moreover, the Rose Bengal staining was localized to the site of the corneal defect, indicating that the mucin layer was only disrupted at the site of the cornea defect (Fig. 4A).

TABLE 1. Corneal Defects in TSP1$^{-/-}$, TLR2$^{-/-}$, and CD36$^{-/-}$ Mice

		Severity of Defect*		
Mouse Strain	Age (mo)	No Defect	Mild Defect	Severe Defect
CD36$^{-/-}$ knockout*	2–6	31	2	1
	8–11	22	11	3
	16	0	12	8†
TSP1$^{-/-}$ knockout‡	2–6	40	0	0
	8–11	43	0	0
TLR2$^{-/-}$ knockout§	19–25	8	0	0

* Data presented in Figure 1 and summarized here, n = 90.

† Frequency of severe defects was compared using Fisher's exact test between (1) CD36$^{-/-}$ mice 16 months old with TLR2$^{-/-}$ mice 19–25 years old ($P = 6.4 \times 10^{-7}$), and (2) CD36$^{-/-}$ mice 8–11 months old with TSP1$^{-/-}$ mice 8–11 months old ($P = 3.1 \times 10^{-6}$).

‡ n = 83.

§ n = 8.

LC-Biotin Staining in CD36$^{-/-}$ Mice

Tight junctions located in the superficial layer of the corneal epithelium act as a physical barrier to invading microorganisms. The integrity of the epithelial tight junctions was tested using a surface biotinylation (LC-biotin) method. This method makes use of a small compound (EZ-Link Sulfo-NHS-LC-Biotin) that normally does not penetrate the epithelial tight junctions.[12,24,25] Therefore, where the tight junctions are intact, LC-biotin will biotinylate only the primary amines on the corneal surface.[12,13] By contrast, when the junctions are disrupted, the compound passes between cells and stains the stroma. The LC-biotin stain did not penetrate into the epithelium in either normal WT C57BL/6 or clear CD36$^{-/-}$ corneas, indicating that the tight junctions are intact (Fig. 4B). By contrast, LC-biotin penetrated the epithelium in corneas of CD36$^{-/-}$ mice with either mild or severe defects. Interestingly, the LC-biotin staining of the corneas with mild defects reveals a detachment of the basal epithelium from the basement membrane, suggesting a possible defect in cell adherence. In conclusion, the LC-biotin staining in corneas with mild defects demonstrates that, in the absence of CD36, a breakdown in the corneal barriers precedes the development of bacterial keratitis.

Bacterial Binding to Corneas of CD36$^{-/-}$ Mice

A critical step in the development of bacterial keratitis is the binding of bacteria to the cornea. Under normal conditions, the mucin barrier prevents bacterial binding, and the epithelial cell tight junctions block bacteria from entering the cornea.[26,27] Because these barriers are disrupted in CD36$^{-/-}$ mice, we next determined whether there is increased bacterial binding to CD36$^{-/-}$ corneas with mild defects. To analyze bacterial binding, GFP-expressing *S. aureus* was incubated with corneas with mild defects. Eyes from WT C57BL/6 mice and CD36$^{-/-}$

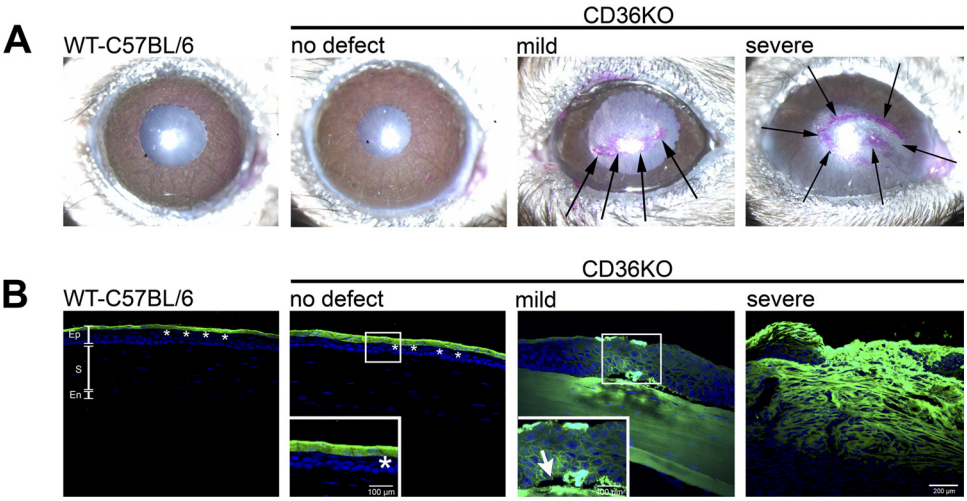

FIGURE 4. The epithelial barrier function in the corneas of CD36$^{-/-}$ mice. (**A**) Rose Bengal staining was performed on WT-C57BL/6 mice and CD36$^{-/-}$ mice with different defects. Rose Bengal stains positive (*pink*) for disrupted mucin layers. (**B**) Epithelial tight junctions were examined with LC-biotin. Intact epithelial tight junctions prevent LC-biotin from penetrating the cornea and staining the stroma (WT-C567BL/6 and CD36$^{-/-}$ mice with no defect). Disrupted epithelial tight junctions allow LC-biotin to penetrate and stain the stroma (CD36$^{-/-}$ mice with mild and severe defects). All sections were counterstained with a cyanine nucleic acid stain (*blue nuclei*) and analyzed via confocal microscopy. Pictures are representative of five mice per group. Ep, epithelium; S, stroma; En, endothelium. *Black arrows* identify the positive Rose Bengal staining in CD36$^{-/-}$ corneas with mild and severe defects. *Asterisks* identify the LC-biotin (*green*) sitting on top of an intact epithelial barrier in WT-C57BL/6 and young CD36$^{-/-}$ mice with no defect. *White arrow* identifies epithelial detachment from the basement membrane.

mice with clear corneas were used as negative controls. As a positive control, GFP-expressing *S. aureus* was added to WT-C57BL/6 eyes with a corneal epithelium debridement wound (data not shown). Confocal analysis revealed no bacterial binding to corneas of WT-C57BL/6 mice and CD36$^{-/-}$ knockout mice without any corneal defects (Fig. 5B). However, significant binding of GFP-expressing *S. aureus* was observed in CD36$^{-/-}$ mice with mild defects, and the binding was confined to the defect. These data indicate that the breakdown of the barriers in the corneas with mild defects coincided with increased bacterial binding. Moreover, this increased susceptibility to bacterial binding in CD36$^{-/-}$ precedes the development of bacterial keratitis.

DISCUSSION

The cornea has multiple barriers that make it highly resistant to bacterial keratitis. This resistance became apparent when researchers in the past attempted to develop animal models of bacterial keratitis. Several in vivo models were developed, using rabbits,[28] mice,[29] and guinea pigs.[30] However, each of these models required either epithelial wounding[28,29,31] or intrastromal injection of bacteria[32] to induce a successful infection. Furthermore, although each of these techniques induced bacterial keratitis, large nonphysiological amounts of bacteria ($1–4 \times 10^8$ CFUs) were also required in addition to a corneal wound.[20,29] The administration of a small amount of bacteria to a corneal wound routinely failed to induce an infection. Herein, we describe the first report of spontaneous bacterial keratitis occurring in mice. Not surprisingly, keratitis only developed after a breakdown in the epithelial barriers, indicating the importance these physical defense mechanisms in preventing infection.

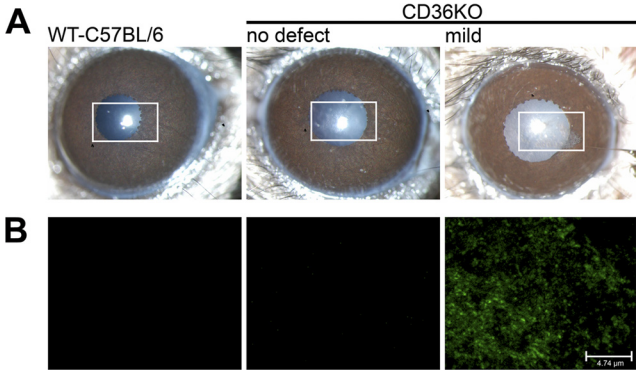

FIGURE 5. Bacterial binding to corneal defects. (**A**) Slit lamp pictures of eyes of WT-C57BL/6 mice and CD36$^{-/-}$ mice without and with mild corneal defects. (**B**) The corneas displayed were recovered and incubated in vivo with GFP-expressing *S. aureus*. Corneas were then washed and examined by confocal microscopy for fluorescent bacteria. Images are representative of at least three different mice per group.

Our study identifies CD36 as a critical component of the corneal epithelial barrier to infection. In the absence of CD36, the mucin layer and epithelial tight junctions break down with age, allowing a member of the normal flora (*S. xylosus*) to bind and penetrate the cornea resulting in spontaneous bacterial keratitis. Although *Staphylococcus* is one of the most common causes of bacterial keratitis in humans, it is considered an opportunistic pathogen, inducing keratitis only when one or more of the corneal barriers are breached.[20] Our study identifies a novel function for CD36 in maintaining the corneal barriers to infection and preventing bacterial keratitis induced by normal flora. Moreover, this novel function of CD36 is independent of TSP1 and TLR2, because TSP1$^{-/-}$ and TLR2$^{-/-}$ mice failed to develop spontaneous keratitis.

CD36 is a member of the class B scavenger receptor family with multiple functions. Beutler and colleagues[33] were the first to identify CD36 as a receptor of microbial diacylglycerides. Moreover, they demonstrated that "oblivious" mice expressing a mutant form of CD36 were unable to clear an intradermal and/or intravenous *S. aureus* inoculum.[33] This inability to clear a *Staphylococcus* inoculation coincided with reduced macrophage function as determined by TNFα production. Stuart and colleagues[7] demonstrated that induction of the innate immune response to *S. aureus* requires CD36-mediated phagocytosis, which triggers TLR2/6 signaling. The function of CD36 is analagous to the LPS receptor, CD14, which clusters the LPS on the cell surface where it engages with TLR2/6.[7] Similarly, CD36 recognizes *S. aureus* and its cell wall component LTA and clusters LTA at the cell surface, where it engages with TLR2/6. Unlike CD14, however, CD36 can also phagocytose *S. aureus* and LTA, concentrating them in the endosome where they again engage TLR2/6. In the absence of CD36, macrophages

display a reduced ability to phagocytose bacteria, resulting in a failure to activate the TLR2 signaling pathway.[7] Therefore, knocking out either CD36 or TLR2 resulted in a significantly reduced protective innate immune response to an intravenous challenge of *S. aureus*.

By contrast, the primary function of CD36 in the cornea appears to be maintaining the physical barriers that prevent bacterial binding. Intravenous injection of 10^{-7} CFUs of *S. aureus* resulted in the death of 50% of CD36$^{-/-}$ mice compared with 0% of WT mice.[7] However, we demonstrated that young CD36$^{-/-}$ mice (without any cornea defect) show no increased susceptibility to *S. aureus*–induced keratitis when as much as 10^{-8} CFUs of *S. aureus* was added to an intact cornea. Only after the development of the cornea defects did CD36$^{-/-}$ mice display increased binding of bacteria at the site of the defect. Moreover, TLR2$^{-/-}$ mice did not develop either corneal defects or spontaneous bacterial keratitis, indicating the corneal pathology observed in CD36$^{-/-}$ mice was due to the role of CD36 in barrier function and not innate immunity. In agreement with our study, Beutler and colleagues[33] reported in supplementary data that aged "oblivious" mice (that had not received a bacterial inoculation) developed spontaneous endophthalmitis. As endophthalmitis was not the focus of their study, these investigators examined only a small number of aged "oblivious" mice and did not examine the corneas of these mice at an earlier stage of their infection (BRK, personal communication with Bruce Beutler, 2006). Therefore, they could not rule out a bacterial keratitis as the initial infection in the eye. Taken together with our current studies, we propose the endophthalmitis reported by Beutler and colleagues[33] was actually secondary to an initial bacterial keratitis caused by a breakdown in the cornea allowing the bacteria to adhere to the corneal surface.

Hardy and colleagues[4] reported that an additional function of CD36 in the cornea was to maintain the avascularity of the cornea. In a mouse model of inflammatory corneal neovascularization, they demonstrated that CD36 inhibits corneal neovascularization directly by inhibiting vessel outgrowth and indirectly by inhibiting macrophage-derived VEGF-A expression.[4] The authors went on to demonstrate that CD36$^{-/-}$ mice developed age-dependent corneal neovascularization accompanied by increased expression of angiogenic factors and inflammation.[5] However, the cause of inflammation in these older mice was unclear. Interestingly, we demonstrate that before the development of neovascularization, CD36$^{-/-}$ mice develop a mild corneal defect that is characterized by a breakdown in the mucin layer, a loss of epithelial tight junctions, and a mild macrophage infiltration into the stroma underlying the epithelial defect. Furthermore, in vitro, we observed increased bacterial binding to the area within the mild defect. Together, this suggests that the inflammation and neovascularization observed by Hardy and colleagues is secondary to the breakdown of the corneal epithelium and subsequent binding of normal flora.

Strict regulation of cell migration and adhesion is critical in the homeostasis and wound repair of the corneal epithelium. Several studies implicate CD36 in both cell adhesion and migration through interactions with actin, collagen, thrombospondin, and $\alpha3\beta1$ and $\alpha6\beta1$ integrins.[34–38] Interestingly, collagen and thrombospondin are major components of the corneal epithelial basement membrane,[39] while both $\alpha3\beta1$ and $\alpha6\beta1$ integrins are constitutively expressed in the basal epithelium of the cornea where they mediate cell attachment to matrix proteins in the basement membrane.[40] Cellular migration is a complex process involving cell-to-matrix and cell-to-cell adhesion and in the cornea in particular, the epithelium must move as an intact sheet to maintain the barrier function.[41] Taken together, these data suggest a novel function for CD36 in maintaining the structural integrity of the corneal epithelial cell sheet as the cells continually migrate to replace the outermost shed layer. In addition, attachment to the basement membrane is critical for the survival of adherent cells and epithelial cells that detach from their underlying basement membrane undergo apoptosis.[42–44] The LC-biotin staining of our CD36$^{-/-}$ corneas with mild defects reveal a detachment of the basal epithelium from the basement membrane coinciding with the loss of tight junctions, suggesting a defect in cell adhesion may underlie the formation of the mild corneal defects. However, the development of the mild defect also coincides with a mild infiltrate of macrophages into the underlying stroma. Infiltrating macrophages have the ability to secrete a variety of matrix metalloproteinases (MMPs) that digest extracellular matrix and integrins. In particular MMP2 and MMP9 are known to cleave specifically type 4 collagen, which is a major structural component of the basement membrane.[45,46] Therefore, we cannot rule out that an early infiltration of macrophages secreting MMPs does not contribute to the detachment of the corneal epithelium and loss of epithelial tight junctions. In vitro experiments are currently underway to determine whether corneal epithelial cells that lack CD36 exhibit defective adhesion and migration properties.

Interestingly, although CD36$^{-/-}$ mice lack CD36 from birth, development of the corneal defects and subsequent spontaneous keratitis occurs only in aged mice. This suggests that early in life other factors and/or pathways compensate for the loss of CD36. However, there are numerous age-related changes that occur in the cornea, resulting in increased cell senescence, increased epithelial permeability, decreased expression of adhesion molecules, and diminished epithelial adhesion to the basal lamina.[47] More important, we predict age-related changes in the cornea coincide with decreased efficiency in compensatory mechanisms. For these reasons we believe the corneal pathogenesis associated with CD36 deficiency becomes apparent only with age and occurs in the central cornea where exposure to environmental insults is the greatest.

In conclusion, our data suggest a novel function for CD36 in the maintenance of the corneal epithelial barriers to infection. In the absence of CD36, the epithelial barrier and mucin layer are disrupted, allowing the normal corneal flora to bind and promoting the development of bacterial keratitis. This is the first report of spontaneous bacterial keratitis in a mouse.

Acknowledgments

The authors thank Marie Ortega and Michelle Mammolenti for their excellent assistance with animal breeding, Don Pottle for technical assistance with Confocal Analysis, and Pablo Argüeso for assistance with Rose Bengal staining.

References

1. Ricciuto J, Heimer SR, Gilmore MS, Argueso P. Cell surface O-glycans limit Staphylococcus aureus adherence to corneal epithelial cells. *Infect Immun.* 2008;76:5215–5220.
2. Yi X, Wang Y, Yu FS. Corneal epithelial tight junctions and their response to lipopolysaccharide challenge. *Invest Ophthalmol Vis Sci.* 2000;41:4093–4100.
3. Febbraio M, Hajjar DP, Silverstein RL. CD36: a class B scavenger receptor involved in angiogenesis, atherosclerosis, inflammation, and lipid metabolism. *J Clin Invest.* 2001;108:785–791.
4. Mwaikambo BR, Sennlaub F, Ong H, Chemtob S, Hardy P. Activation of CD36 inhibits and induces regression of inflammatory corneal neovascularization. *Invest Ophthalmol Vis Sci.* 2006;47:4356–4364.
5. Mwaikambo BR, Sennlaub F, Ong H, Chemtob S, Hardy P. Genetic ablation of CD36 induces age-related corneal neovascularization. *Cornea.* 2008;27:1037–1041.

6. Moore KJ, El Khoury J, Medeiros LA, et al. A CD36-initiated signaling cascade mediates inflammatory effects of beta-amyloid. *J Biol Chem.* 2002;277:47373–47379.
7. Stuart LM, Deng J, Silver JM, et al. Response to Staphylococcus aureus requires CD36-mediated phagocytosis triggered by the COOH-terminal cytoplasmic domain. *J Cell Biol.* 2005;170:477–485.
8. Agah A, Kyriakides TR, Lawler J, Bornstein P. The lack of thrombospondin-1 (TSP1) dictates the course of wound healing in double-TSP1/TSP2-null mice. *Am J Pathol.* 2002;161:831–839.
9. Beveridge TJ. Use of the gram stain in microbiology. *Biotech Histochem.* 2001;76:111–118.
10. Cox CR, Gilmore MS. Native microbial colonization of Drosophila melanogaster and its use as a model of Enterococcus faecalis pathogenesis. *Infect Immun.* 2007;75:1565–1576.
11. Toshida H, Nguyen DH, Beuerman RW, Murakami A. Evaluation of novel dry eye model: preganglionic parasympathetic denervation in rabbit. *Invest Ophthalmol Vis Sci.* 2007;48:4468–4475.
12. Xu KP, Li XF, Yu FS. Corneal organ culture model for assessing epithelial responses to surfactants. *Toxicol Sci.* 2000;58:306–314.
13. Hutcheon AE, Sippel KC, Zieske JD. Examination of the restoration of epithelial barrier function following superficial keratectomy. *Exp Eye Res.* 2007;84:32–38.
14. Cheung AL, Nast CC, Bayer AS. Selective activation of sar promoters with the use of green fluorescent protein transcriptional fusions as the detection system in the rabbit endocarditis model. *Infect Immun.* 1998;66:5988–5993.
15. Schmuth M, Ortegon AM, Mao-Qiang M, Elias PM, Feingold KR, Stahl A. Differential expression of fatty acid transport proteins in epidermis and skin appendages. *J Invest Dermatol.* 2005;125:1174–1181.
16. Harris IR, Farrell AM, Memon RA, Grunfeld C, Elias PM, Feingold KR. Expression and regulation of mRNA for putative fatty acid transport related proteins and fatty acyl CoA synthase in murine epidermis and cultured human keratinocytes. *J Invest Dermatol.* 1998;111:722–726.
17. Hazlett LD, McClellan S, Kwon B, Barrett R. Increased severity of Pseudomonas aeruginosa corneal infection in strains of mice designated as Th1 versus Th2 responsive. *Invest Ophthalmol Vis Sci.* 2000;41:805–810.
18. Girgis DO, Sloop GD, Reed JM, O'Callaghan RJ. A new topical model of Staphylococcus corneal infection in the mouse. *Invest Ophthalmol Vis Sci.* 2003;44:1591–1597.
19. Kloos WE, Zimmerman RJ, Smith RF. Preliminary studies on the characterization and distribution of Staphylococcus and Micrococcus species on animla skin. *Appl Environ Microbiol.* 1976;31:53–59.
20. Nagase N, Sasaki A, Yamashita K, et al. Isolation and species of staphylococci from animal and human skin. *J Vet Med Sci.* 2002;64:245–250.
21. Argueso P, Tisdale A, Spurr-Michaud S, Sumiyoshi M, Gipson IK. Mucin characteristics of human corneal-limbal epithelial cells that exclude the rose bengal anionic dye. *Invest Ophthalmol Vis Sci.* 2006;47:113–119.
22. Kim J. The use of vital dyes in corneal disease. *Curr Opin Ophthalmol.* 2000;11:241–247.
23. Feenstra RP, Tseng SC. What is actually stained by rose bengal? *Arch Ophthalmol.* 1992;110:984–993.
24. Chen Y, Merzdorf C, Paul DL, Goodenough DA. COOH terminus of occludin is required for tight junction barrier function in early Xenopus embryos. *J Cell Biol.* 1997;138:891–899.
25. Merzdorf CS, Chen YH, Goodenough DA. Formation of functional tight junctions in Xenopus embryos. *Dev Biol.* 1998;195:187–203.
26. Mantelli F, Argueso P. Functions of ocular surface mucins in health and disease. *Curr Opin Allergy Clin Immunol.* 2008;8:477–483.
27. Huang AJ, Tseng SC, Kenyon KR. Paracellular permeability of corneal and conjunctival epithelia. *Invest Ophthalmol Vis Sci.* 1989;30:684–689.
28. Hume EB, Dajcs JJ, Moreau JM, Sloop GD, Willcox MD, O'Callaghan RJ. Staphylococcus corneal virulence in a new topical model of infection. *Invest Ophthalmol Vis Sci.* 2001;42:2904–2908.
29. Hume EB, Cole N, Khan S, et al. A Staphylococcus aureus mouse keratitis topical infection model: cytokine balance in different strains of mice. *Immunol Cell Biol.* 2005;83:294–300.
30. Chusid MJ, Davis SD. Experimental bacterial keratitis in neutropenic guinea pigs: polymorphonuclear leukocytes in corneal host defense. *Infect Immun.* 1979;24:948–952.
31. Zieske JD, Higashijima SC, Spurr-Michaud SJ, Gipson IK. Biosynthetic responses of the rabbit cornea to a keratectomy wound. *Invest Ophthalmol Vis Sci.* 1987;28:1668–1677.
32. Sloop GD, Moreau JM, Conerly LL, Dajcs JJ, O'Callaghan RJ. Acute inflammation of the eyelid and cornea in Staphylococcus keratitis in the rabbit. *Invest Ophthalmol Vis Sci.* 1999;40:385–391.
33. Hoebe K, Georgel P, Rutschmann S, et al. CD36 is a sensor of diacylglycerides. *Nature.* 2005;433:523–527.
34. Park YM, Febbraio M, Silverstein RL. CD36 modulates migration of mouse and human macrophages in response to oxidized LDL and may contribute to macrophage trapping in the arterial intima. *J Clin Invest.* 2009;119:136–145.
35. Stuart LM, Bell SA, Stewart CR, et al. CD36 signals to the actin cytoskeleton and regulates microglial migration via a p130Cas complex. *J Biol Chem.* 2007;282:27392–27401.
36. Tandon NN, Kralisz U, Jamieson GA. Identification of glycoprotein IV (CD36) as a primary receptor for platelet-collagen adhesion. *J Biol Chem.* 1989;264:7576–7583.
37. Barnwell JW, Asch AS, Nachman RL, Yamaya M, Aikawa M, Ingravallo P. A human 88-kD membrane glycoprotein (CD36) functions in vitro as a receptor for a cytoadherence ligand on Plasmodium falciparum-infected erythrocytes. *J Clin Invest.* 1989;84:765–772.
38. Thorne RF, Marshall JF, Shafren DR, Gibson PG, Hart IR, Burns GF. The integrins alpha3beta1 and alpha6beta1 physically and functionally associate with CD36 in human melanoma cells. Requirement for the extracellular domain OF CD36. *J Biol Chem.* 2000;275:35264–35275.
39. Maguen E, Zorapapel NC, Zieske JD, et al. Extracellular matrix and matrix metalloproteinase changes in human corneas after complicated laser-assisted in situ keratomileusis (LASIK). *Cornea.* 2002;21:95–100.
40. Stepp MA. Corneal integrins and their functions. *Exp Eye Res.* 2006;83:3–15.
41. Zelenka PS, Arpitha P. Coordinating cell proliferation and migration in the lens and cornea. *Semin Cell Dev Biol.* 2008;19:113–124.
42. Frisch SM, Francis H. Disruption of epithelial cell-matrix interactions induces apoptosis. *J Cell Biol.* 1994;124:619–626.
43. Grossmann J. Molecular mechanisms of "detachment-induced apoptosis–Anoikis." *Apoptosis.* 2002;7:247–260.
44. Valentijn AJ, Zouq N, Gilmore AP. Anoikis. *Biochem Soc Trans.* 2004;32:421–425.
45. Corotti MV, Zambuzzi WF, Paiva KBS et al. Immunolocalization of matrix metalloproteinases-2 and -9 during apical periodontitis development. *Arch Oral Biol.* 2009;54:764–771.
46. Visse R and Nagase H. Matrix metalloproteinases and tissue inhibitors of metalloproteinases: structure, function, and biochemistry. *Circ Res.* 2003;92:827–839.
47. Chang SW, Hu FR. Changes in corneal autofluorescence and corneal epithelial barrier function with aging. *Cornea*. 1993;12:493–499.